Title

High-Resolution Fourier-Domain Optical Coherence Tomography of Choroidal Neovascular Membranes Associated with Age-Related Macular Degeneration

Journal

Investigative Ophthalmology & Visual Science, 51(8)

ISSN

0146-0404

Authors

Park, Susanna S
Truong, Steven N
Zawadzki, Robert J
et al.

Publication Date

2010-08-01

DOI

10.1167/iovs.09-4256

Peer reviewed

High-Resolution Fourier-Domain Optical Coherence Tomography of Choroidal Neovascular Membranes Associated with Age-Related Macular Degeneration

Susanna S. Park, Steven N. Truong, Robert J. Zawadzki, Suhail Alam, Stacey S. Choi, David G. Telander, John S. Werner, and Lawrence S. Morse

Purpose. To investigate the use of high-resolution Fourier-domain optical coherence tomography (Fd-OCT) to image choroidal neovascular membranes (CNVMs) associated with exudative age-related macular degeneration (eAMD).

Methods. An Fd-OCT instrument with axial resolution of 4 to 4.5 μm and transverse resolution of 10 to 15 μm was used to image 21 eyes (19 subjects) with newly diagnosed eAMD. A raster series of 100 B-scans separated by 60 μm was used to study the growth pattern of CNVM and associated morphologic changes. CNVM size was determined using 250 to 300 serial virtual C-scans of reconstructed three-dimensional macular volume.

Results. A highly reflective subretinal and/or subretinal pigment epithelial (RPE) lesion that co-localized with the CNVM seen on fluorescein angiography was detected in all eyes by Fd-OCT. Although a combined subretinal and sub-RPE growth pattern of various degrees was noted in 15 (71%) eyes, a statistically significant difference in the distribution of growth pattern was noted when classic CNVM was compared with occult CNVM ($\chi^2 = 10.4$, $df = 2$, $P < 0.005$). Classic lesions had >90% subretinal growth pattern, whereas occult lesions had a more variable growth pattern. Angiographic CNVM size correlated with size on Fd-OCT but correlation was better for classic CNVM (classic, $r = 0.99$, $P < 0.0001$; nonclassic, $r = 0.78$, $P < 0.001$).

Conclusions. Fd-OCT is a promising potential alternative modality to visualize CNVM with AMD. Angiographic lesion size and type correlated with growth pattern and size of CNVM on Fd-OCT, with correlation being stronger for classic lesions. (*Invest Ophthalmol Vis Sci.* 2010;51:4200–4206) DOI:10.1167/iovs.09-4256

From the Department of Ophthalmology and Vision Science, Davis Medical Center, University of California, Sacramento, California.

Presented in part at the Annual Meeting of the American Society of Retinal Specialists, Maui, HI, October 2008, and at the annual meeting of the American Academy of Ophthalmology, Atlanta, GA, November 9, 2008.

Supported by Grant EY014743 (JSW) from the National Eye Institute, Bethesda, MD, and an unrestricted departmental grant from Research to Prevent Blindness (RPB), New York, NY. JSW is the recipient of an RPB Senior Scientist Award.

Submitted for publication July 1, 2009; revised January 12, 2010; accepted February 14, 2010.

Disclosure: **S.S. Park**, None; **S.N. Truong**, None; **R.J. Zawadzki**, None; **S. Alam**, None; **S.S. Choi**, None; **D.G. Telander**, None; **J.S. Werner**, None; **L.S. Morse**, None

Corresponding author: Susanna S. Park, Department of Ophthalmology and Vision Science, University of California Davis Medical Center, 4860 Y Street, Suite 2400, Sacramento, CA 95817; susanna.park@ucdmc.ucdavis.edu.

Exudative age-related macular degeneration (eAMD) is a leading cause of irreversible blindness in the elderly in the United States.[1] The anatomy and growth patterns of choroidal neovascular membranes (CNVM) associated with eAMD have been studied in the past using either enucleated eyes or excised tissue from submacular surgery, in an attempt to understand the pathogenesis of this condition.[2–14] These studies have demonstrated that CNVM comprises a dynamic proliferation of fibrovascular tissue through Bruch's membrane. Gass[8] used enucleated eyes and classified the neovascular growth pattern as subretinal pigment epithelial (RPE) (type 1), subretinal (type 2), or combined.

Several studies attempted to demonstrate a correlation between the angiographic classification of CNVM (classic versus occult) and the anatomic classification (type 1 vs. type 2). However, data on postmortem eyes are limited.[10,11] Several groups have reported on clinicopathologic correlation using surgically removed CNVMs. These reports showed that classic CNVMs tend to exhibit either a combined or subretinal growth pattern while occult CNVMs tend to be composed of tissue that appeared to be from the sub-RPE space.[12–14] However, tissue classification of surgically removed CNVMs can have limited accuracy since anatomy is disrupted, and incomplete excision of CNVM during surgery cannot be ruled out.

With the emergence of optical coherence tomography (OCT), a new method for studying CNVM growth patterns in living subjects became available. OCT provides a noninvasive, nondestructive method of obtaining detailed anatomic data in vivo. A study using the commercially available time-domain OCT system Stratus OCT (Carl Zeiss Meditec, Inc., Dublin, CA) suggested that classic CNVM tends to be subretinal whereas occult CNVM tends to be sub-RPE.[15,16] However, the Stratus OCT system that was used provides only six radial scans of the macula and has limited axial and transverse resolution. Thus, it is not possible to visualize the whole extent of the CNVM with this instrument.

Fourier-domain OCT (Fd-OCT) systems are newer generation instruments that allow a reduction in image acquisition time by an additional factor of 20 to 40 when compared with the Stratus OCT. These modifications allow acquisition of rapid serial fine-cut B-scans of the macula in a single scanning sweep, so that the entire macula can be imaged and analyzed.[17,18] The new Fd-OCT system has allowed detailed imaging of macular lesions that may be missed with the time-domain OCT system.[17] There are several recent reports using Fd-OCT to image eyes with eAMD. These reports have concentrated on improved visualization of the retinal layers and drusen in eyes with eAMD before and after treatment with inhibitors of vascular endothelial growth factor when compared to the traditional time-domain OCT.[19–23] One report describes volume measurements of CNVM before and after treatment but did not mention the growth pattern of CNVM.[24]

Investigative Ophthalmology & Visual Science, August 2010, Vol. 51, No. 8

In this report, a high-resolution Fd-OCT system developed at our institution was used to image eyes with newly diagnosed eAMD to evaluate the usefulness of this instrument in visualizing CNVM and associated morphologic changes.

Materials and Methods

This prospective observational case series enrolled 21 eyes of 19 patients (8 men, 11 women; 48–92 years of age) with newly diagnosed eAMD seen in the Retina Clinic at the University of California Davis Eye Center between September 2005 and June 2006. For this study, eyes diagnosed with retinal angiomatous proliferation or concurrent macular hemorrhage that may obscure part of the CNVM on fluorescein angiography (FA) were excluded. Informed written consent was obtained from all patients before enrollment. This study was approved by the Institutional Review Board of the University of California, Davis School of Medicine and was conducted in compliance with the Declaration of Helsinki.

All patients underwent a dilated fundus examination, fundus photography, and standard FA. Each angiogram was independently evaluated by five retinal specialists (SNT, SA, DGT, LSM, SSP) and classified according to the Macular Photocoagulation Study protocol as classic, minimally classic, occult with late leakage of undetermined source, or occult with pigment epithelial detachment (PED; i.e., fibrovascular PED).[25] For the minimally classic lesions, the classic and occult components were quantified. In rare cases when angiogram interpretation varied among reviewers, the angiogram was reviewed as a group to reach consensus. The CNVMs were then outlined and the GLD was measured (IMAGEnet 2000 ver. 2.55; Topcon America Corp., Paramus, NJ). For fibrovascular PED, the entire lesion (including area of PED) was included.

A state-of-the-art Fd-OCT system similar to that described by Wojtkowski et al.[26] and further improved by Nassif et al.[27] was used to image all 21 eyes on the same day as FA. This system was constructed at the University of California, Davis Medical Center.[18] The instrument used a superluminescent diode as a light source (855 nm at 7 nm bandwidth; model D855; Superlum Diodes Ltd., Moscow, Russia), and created images with an axial resolution of 4 to 4.5 μm, and calculated transverse resolution between 10 and 15 μm. A raster series of 100 B-scans (1000 A-scans/frame, nine frames/s) imaged over a $6 \times 6 \times$ 2-mm volume of retina and underlying RPE (lateral $\times$ lateral $\times$ depth) centered over the macula was obtained. The total acquisition time for a single macular sweep was 11 seconds. Each consecutive B-scan image was laterally separated by 60 μm on the retina. After the 100 B-scans were acquired, the images were registered by using custom software to minimize fine axial motion artifacts. After careful inspection and manual correction of registration, the B-scans were shifted and rotated to reduce axial shift.

Each single B-scan image was analyzed to carefully identify the CNVM. CNVM appeared on the gray-scale B-scan Fd-OCT images as a highly reflective lesion in the subretinal space, sub-RPE space, or both.[17,22,24,28] A CNVM that was localized predominantly (>90% of the lesion) in the subretinal space on Fd-OCT was classified as type 2. A CNVM that was identified predominantly (>90% of the lesion) in the sub-RPE space was classified as type 1. Any CNVM that was not found predominantly (>90%) in the subretinal or sub-RPE space was classified as combined. The serial B-scan Fd-OCT images of each subject were independently analyzed by five retinal specialists (SNT, SA, DGT, LSM, SSP) who were blinded to the angiographic classification of the lesion at the time of review. In rare cases of disagreement among the retinal specialists, the Fd-OCT images were reviewed as a group until consensus was reached. The serial B-scan Fd-OCT images were reviewed also for the presence of cystoid macular edema (CME), subretinal fluid (SRF) or PED. PED on Fd-OCT B-scans was identified by elevation of the RPE layer over a hyporeflective space and did not include elevation of the RPE layer over hyperreflective lesions suggestive of CNVM or drusen.

The images of the macula were then reconstructed into a three-dimensional (3-D) volume by using custom software developed in collaboration with the Institute for Data Analysis and Visualization (IDAV), University of California, Davis. From this 3-D structure of the macula, a series of 250 to 300 en face images (C-scans), axially separated by 3 μm, was then created (Fig. 1C) with custom software. Each C-scan was carefully analyzed to localize and measure the CNVM with ImageJ software (developed by Wayne Rasband, and provided in the public domain by National Institutes of Health, Bethesda, MD; available at http://rsb.info.nih.gov/ij/index.html). In some eyes with myopia, the Fd-OCT images were flattened with respect to Bruch's membrane to minimize the effect of the globe curvature on the C-scan.[29] By using the pixel measuring function of the ImageJ software, the number of pixels used by the lesion was counted, and the number of pixels was coverted to micrometers by an investigator (ST) who was blinded to the GLD of the lesion obtained with FA. In most cases, a single C-scan that depicted the GLD of the lesion could be used. In a few cases, two or more serial C-scans were overlaid to accurately obtain the GLD of the CNVM (Fig 1). The specific C-scan with the GLD lesion outlined was then overlaid onto an FA image (Photoshop CS; Adobe Systems Inc., San Jose, CA), as previously described.[29,30] Alignment was achieved by using visible landmarks, such as vessel bifurcations, as reference points. The C-scan was scaled and rotated to achieve accurate correspondences of the reference points between the two images, as previously described.

The angiographic classification and size of CNVMs were compared with the anatomic growth pattern and size of CNVMs noted on Fd-OCT (Stat View ver. 5.0.1; SAS Institute, Cary, NC).

Results

Among 21 eyes of 19 patients with newly diagnosed eAMD that met the inclusion and exclusion criteria of this study and were imaged with Fd-OCT, a highly reflective subretinal and/or sub-RPE lesion was visualized in the macula of all 21 eyes by Fd-OCT. These lesions co-localized to the area of CNVM seen on FA. Table 1 lists the demographic information, the angiographic classification of CNVM, and the Fd-OCT findings. Of the 21 eyes imaged, FA showed classic CNVM in 7 (33%) eyes, minimally classic CNVM in 3 (14%) eyes and an occult CNVM in 11 (53%) eyes. Among eyes with occult CNVM, seven (33%) had late leakage of undetermined source and four (20%) had fibrovascular PED (i.e., occult CNVM with late irregular pooling into the PED).

By analyzing the 100 serial Fd-OCT B-scans of the macula, we determined the anatomic growth pattern of the CNVM in all but one eye (95%). A combined sub-RPE and subretinal growth pattern of varying degrees was noted in 15 (71%) eyes. However, based on the classification of growth pattern as defined by this study, 7 (33%) eyes had >90% sub-RPE (i.e., type 1) growth patterns, 10 (48%) had >90% subretinal (i.e., type 2) growth pattern, and 3 (14%) had a combined growth pattern (Table 1).

Table 2 summarizes the anatomic growth pattern of the CNVM on Fd-OCT for the various angiographic lesion types. Of the seven eyes that had classic CNVM on FA, >90% subretinal (type 2) growth pattern was observed in six (86%) eyes, and one eye was indeterminant. Among those seven eyes, four had a small sub-RPE component that was <10% of the lesion.

Among 11 eyes with occult CNVM, 7 (64%) had >90% sub-RPE (type 1) growth pattern, 2 had >90% subretinal growth pattern, and 2 had a combined growth pattern. The two eyes with occult CNVMs with >90% subretinal (type 2) growth pattern had fibrovascular PED (Fig. 1).

A statistically significant difference in the distribution of type 1 and 2 growth patterns was noted among eyes with classic CNVM when compared with eyes with occult CNVM

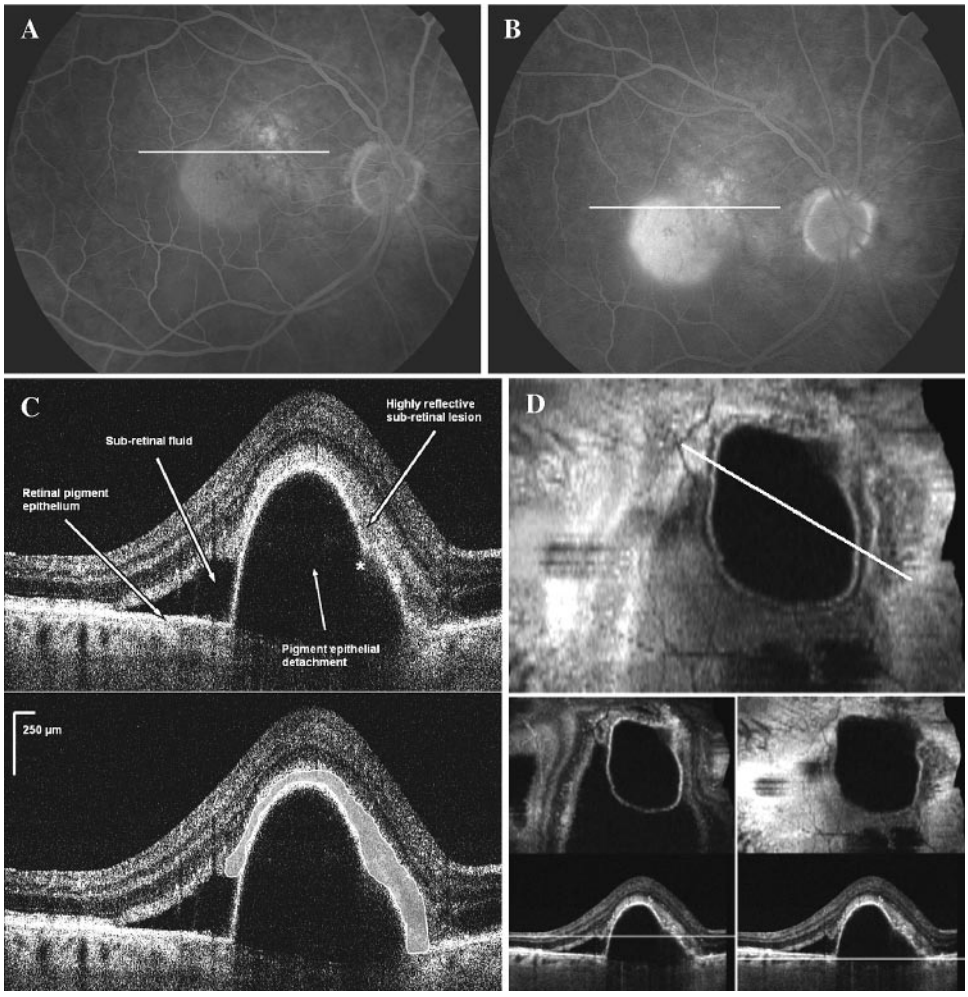

FIGURE 1. FA and high-resolution Fd-OCT of the right eye in case 17 with an occult CNVM associated with a PED from eAMD showing a predominantly subretinal growth pattern of CNVM. (**A**) Early-phase FA shows an ill-defined area of hyperfluorescence centered over the macula with an adjacent area of early pooling consistent with a PED. *White line*: the representative B-scan shown in Figure 2C. (**B**) Late-phase FA showing intense pooling into the PED, with ill-defined leakage at the superonasal edge. *White line*: the representative Fd-OCT B-scan shown in Figure 2C. (**C**) A representative Fd-OCT B-scan shows a large PED with an adjacent area of subretinal fluid. There is a highly reflective subretinal lesion above the PED, consistent with a type 2 (subretinal) CNVM. There is a focal spot of discontinuity in the RPE (✶), with a possible small extension of the hyperreflectivity into the sub-RPE space. The lower image outlines the extent of the hyperreflective lesion. (**D**) Serial reconstructed C-scans were overlaid to measure the GLD of the CNVM (*top image*, *line*). *Bottom*: B-scans, with *white lines* representing the cut depicted by the C-scan shown above.

(χ^2 = 10.4, df = 2, $P < 0.005$)—that is, a type 1, or >90% sub-RPE growth pattern, was more likely to be associated with angiographically occult lesions, whereas type 2, or >90% subretinal growth pattern was more likely associated with classic lesions.

Among the three eyes with minimally classic pattern of leakage on FA, two had a >90% subretinal (type 2) growth pattern (Fig. 2) and one had a combined pattern of growth on Fd-OCT.

Tables 1 and 3 summarize the retinal morphologic changes associated with CNVM as seen on Fd-OCT. Among the seven eyes with classic CNVM, three had associated CME and six had associated SRF visible on Fd-OCT. None of the eyes had PED. Among the seven eyes with occult CNVM without PED, all had CME, five had SRF, and five had PED. On Fd-OCT serial B-scans, all eyes with occult CVNM associated with PED (i.e., fibrovascular PED) on FA had PED on Fd-OCT, two eyes had CME, and three eyes had SRF. There was no statistically significant difference in the distribution of these morphologic changes between eyes with classic CNVM and eyes with occult CNVM (χ^2 = 5.272, df = 4, $P > 0.05$) in this small series. Nonetheless, none of the eyes with classic CNVM had an associated PED on Fd-OCT, whereas 9 of 11 eyes with occult CNVM on FA had PED on Fd-OCT. Of note, 71% of eyes with occult CNVM without PED on FA had PED on Fd-OCT.

Further analysis of possible association of these morphologic changes in the retina with specific growth pattern of CNVM seen on Fd-OCT showed no statistically significant difference in the distribution of CME, SRF, and PED with type 1 or 2 growth pattern of CNVM seen on Fd-OCT (χ^2 = 2.282, df = 4, $P > 0.05$), but the numbers in each group were small.

Virtual C-scan images of the macula were analyzed serially to determine the GLD of the highly reflective subretinal/sub-RPE lesion seen on serial B-scan Fd-OCT images. In most cases, the GLD could be determined by using a single reconstructed C-scan, but in a few cases (Fig. 1D), serial C-scans were overlaid to obtain a two-dimensional image of the CNVM to obtain the GLD. In all eyes, the highly reflective lesion co-localized with the CNVM seen on FA when the C-scan images were overlaid on FA images. As shown in Figure 3A, linear regression analysis showed a strong positive correlation between the size of CNVM (GLD) obtained from Fd-OCT C-scans and the size of CNVM (GLD) on FA in eyes with classic CNVM (n = 7; r = 0.99, $F_{1,5}$ = 214.10, $P < 0.0001$) despite the small number of eyes. The intercept also did not differ significantly from 0 (t = 0.223, P = 0.831), indicating that there was no offset between the two sets of measurements. For eyes with nonclassic CNVM, including eyes with minimally classic CNVM and eyes with occult CNVM with or without PED, Figure 3B shows that the relation between the two measures is not as strong, but was still statistically significant, despite the small sample size (n = 14; r = 0.78, $F_{1,12}$ = 18.44; $P < 0.001$).

DISCUSSION

In this study, a high-resolution Fd-OCT instrument developed in our institution was used to image eyes with newly diagnosed

TABLE 1. Summary of Demographics, Angiographic, and High-Resolution Fd-OCT Findings of CNVM Characteristics Associated with eAMD

Case	Age	Sex	Eye	Lesion Type on FA	CNVM Growth Pattern On Fd-OCT	Morphologic Findings on Fd-Oct	Angiographic CNVM Size, GLD (mm)	Fd-OCT CNVM Size, GLD (mm)
1	79	M	OS	100% Classic	Type 2*	SRF	0.99	0.94
2	82	M	OD	100% Classic	Indeterminate	CME	1.83	1.73
3	65	M	OD	100% Classic	Type 2*	CME, SRF	2.79	2.70
4	88	F	OS	100% Classic	Type 2	CME, SRF	1.91	2.06
5	91	F	OD	100% Classic	Type 2*	SRF	1.24	1.19
6	48	F	OD	100% Classic	Type 2	SRF	1.19	1.23
7	48	F	OS	100% Classic	Type 2*	SRF	2.00	1.89
8	82	M	OS	40% Classic, 60% occult	Type 2*	SRF, PED	1.91	1.87
9	92	F	OD	60% Occult, 40% classic	Type 2	CME	2.46	1.32
10	77	M	OD	70% Occult, 30% classic	Combined	CME, PED	1.21	1.29
11	72	M	OD	Occult with PED†	Type 2*	SRF, PED	4.11	3.68
12	82	F	OS	Occult with PED†	Type 1	CME, SRF, PED	3.41	1.54
13	83	F	OD	Occult with PED†	Type 1	PED	1.34	0.72
14	83	F	OS	Occult with PED†	Type 2	SRF, PED	5.58	2.07
15	74	M	OD	Occult	Type 1‡	CME, SRF, PED	3.60	3.34
16	74	M	OD	Occult	Type 1‡	CME, SRF, PED	4.44	4.40
17	84	M	OS	Occult	Type 1‡	CME, SRF, PED	2.30	2.34
18	84	F	OD	Occult	Type 1‡	CME, PED	6.79	4.31
19	84	F	OD	Occult	Combined	CME, SRF	5.41	3.98
20	76	F	OS	Occult	Type 1	CME, SRF	2.84	2.16
21	92	F	OS	Occult	Combined	CME, PED	1.84	1.61

Type 1, >90% subretinal; Type 2, 90% subretinal.
* Minor type 1 component (<10% lesion) visualized.
† Fibrovascular PED.
‡ Minor type 2 component (<10% lesion) visualized.

eAMD to determine the usefulness of this instrument in visualizing the anatomic growth pattern of CNVM and associated morphologic changes in the macula. This study was limited to eyes with occult and/or classic CNVM on FA, since the growth pattern of neovascular tissue associated with retinal angiomatous proliferation has been described with this Fd-OCT system.[28] The data presented show that Fd-OCT may be a useful tool for visualizing CNVM and characterizing the growth pattern of occult and/or classic CNVMs. Among the 21 eyes imaged, a hyperreflective subretinal and/or sub-RPE lesion consistent with CNVM was identified in all eyes. This lesion colocalized to the area of leakage seen in FA, and the size of CNVM (GLD) measured on FA correlated with that measured with virtual C-scans of Fd-OCT. The correlation was best for the classic lesions, which also tended to be smaller than the nonclassic CNVMs imaged in our study population. Furthermore, Fd-OCT images were of sufficient resolution to enable categorizing of the growth pattern in 95% of the eyes. This result is in contrast to the 65% rate reported recently by the SST (Submacular Surgery Trials) research group, who used histologic methods after submacular surgery.[14] These Fd-OCT images were acquired in vivo in a noninvasive manner on the same day as FA, making the comparison between the two imaging modalities potentially more reliable than histology of surgically excised specimens.

In our study of 21 eyes, 54% of eyes had occult CNVM and 33% of eyes had classic CNVM. When compared with previous reports of 60% to 73% incidence of occult CNVM and 20% to 21% incidence of classic CNVM, our study population had slightly higher proportion of eyes with classic CNVM,[31–33] perhaps because our study excluded eyes with nonclassic lesions associated with RAP or macular hemorrhage. Among the 21 eyes studied, 71% had some degree of combined subretinal and sub-RPE growth pattern of CNVM detected on Fd-OCT. Nonetheless, a statistically significant difference in the distribution of growth pattern was noted when eyes with classic CNVM were compared to eyes with occult CNVM. We found that 86% of eyes with classic CNVM on FA had a >90% subretinal (type 2) growth pattern on Fd-OCT, although many also had a small sub-RPE component that made up less than 10% of the CNVM. These findings are similar to those of the SST study, which described classic CNVM as having a subretinal growth pattern or a combined growth pattern.[14] For eyes with occult CNVM, a more variable growth pattern was noted, although 64% had >90% sub-RPE (type 1) growth pattern. These observations are consistent with the limited histologic data in postmortem eyes that suggest that occult CNVMs tend to exhibit a sub-RPE or combined pattern of growth.[10–14] Most of the eyes with occult CNVM in our study also had a PED visualized on Fd-OCT, although not always appreciated on FA.

TABLE 2. Growth Pattern of Classic and Occult CNVM Due to eAMD as Determined by High-Resolution Fd-OCT

	Classic CNVM (n = 7)	Minimally Classic CNVM (n = 3)	All Occult CNVM (n = 11)	Occult CNVM with PED* (n = 4)	Occult CNVM without PED (n = 7)
Type 1 (>90% sub-RPE)	0	0	7	2	5
Type 2 (>90% subretinal)	6	2	2	2	0
Combined	0	1	2	0	2
Indeterminant	1	0	0	0	0

* Fibrovascular PED.

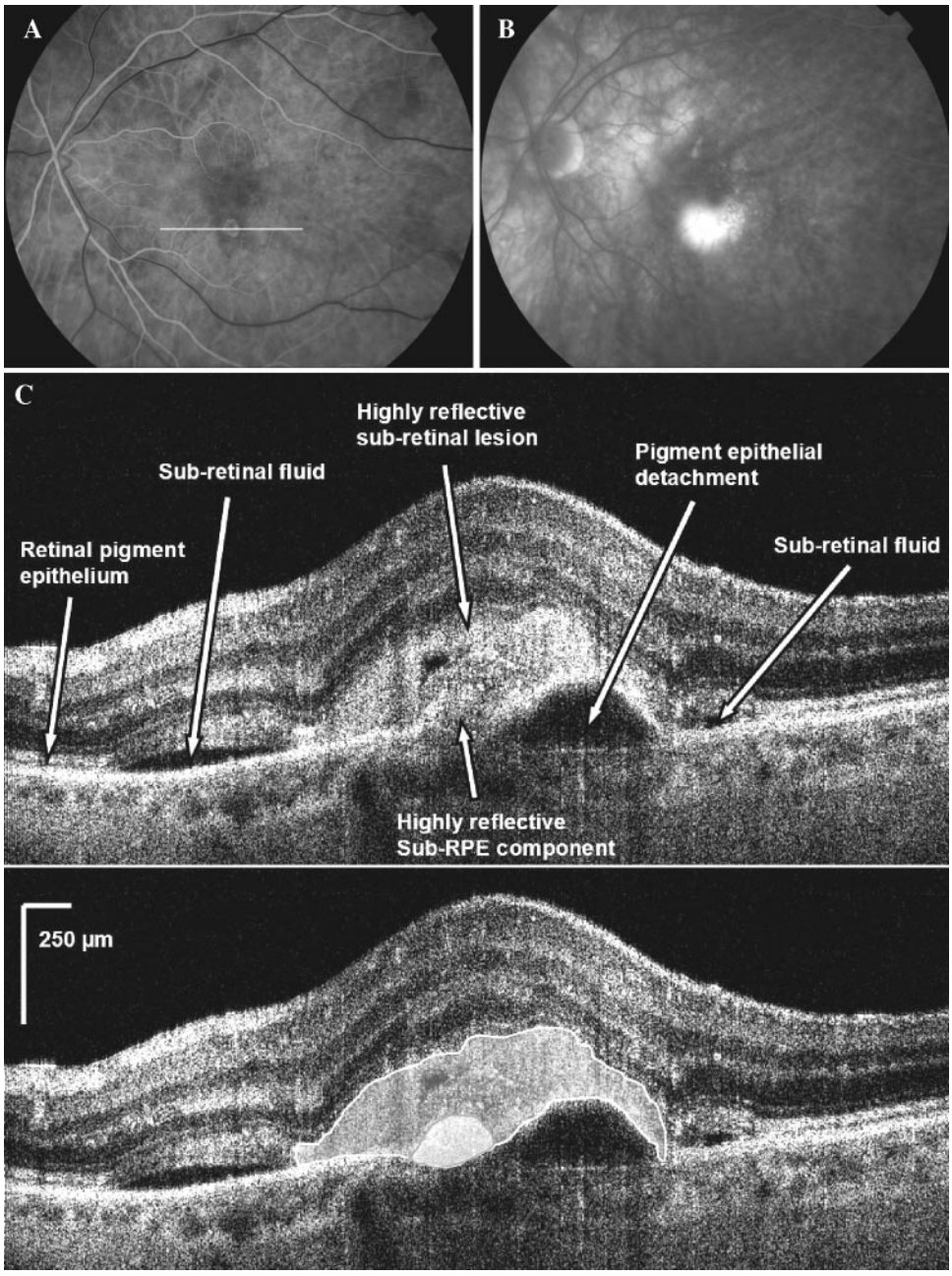

FIGURE 2. Fluorescein angiogram and high-resolution Fd-OCT of the left eye in case 8 showing a mostly subretinal growth pattern of CNVM in an eye with a minimally classic angiographic lesion composition. (**A**) Early phase angiogram shows a well-defined juxtafoveal area of hyperfluorescence with rim of hypofluorescence and an adjacent area of faint mottled hyperfluorescence. *White line*: the representative B-scan shown in Figure 1C. (**B**) Late-phase FA showing leakage around the area of early well-defined hyperfluorescence and the adjacent area of mottled hyperfluorescence, consistent with a minimally classic CNVM. (**C**, *top*) A representative Fd-OCT B-scan selected out of a series of 100 B-scans shows a hyperreflective lesion mostly in the subretinal space, with a small sub-RPE component connected through a focal discontinuity in the RPE within the lesion. There are pockets of subretinal fluid on either side of the lesion, as well as a small PED. *Bottom*: the extent of the hyperreflective lesion is outlined in *gray* with the sub-RPE component of the lesion in a lighter shade.

When occult CNVM was associated with a PED on FA (i.e., fibrovascular PED), the growth pattern of CNVM as determined by Fd-OCT was variable. Two of four eyes with occult CNVM associated with PED on FA demonstrated >90% subretinal (type 2) growth pattern on Fd-OCT although no classic lesion was noted on FA. These cases suggest that, in the presence of significant pooling of fluorescein dye into the PED, the angiographic characteristic of the CNVM may be misleading and may not correlate with the anatomic growth pattern of the CNVM.

TABLE 3. Associated Retinal Findings on High-Resolution Fd-OCT among Eyes with Classic or Occult CNVMe Due to Degeneration in eAMD

	Classic CNVM (n = 7)	Minimally Classic CNVM (n = 3)	All Occult CNVM (n = 11)	Occult CNVM with PED* (n = 4)	Occult CNVM without PED (n = 7)
CME	3 (43)	2 (67)	9 (82)	2 (50)	7 (100)
Subretinal Fluid	6 (86)	1 (33)	8 (73)	3 (75)	5 (71)
PED	0	2 (67)	9 (82)	4 (100)	5 (71)

Data are number of eyes (% of total in group).
* Fibrovascular PED.

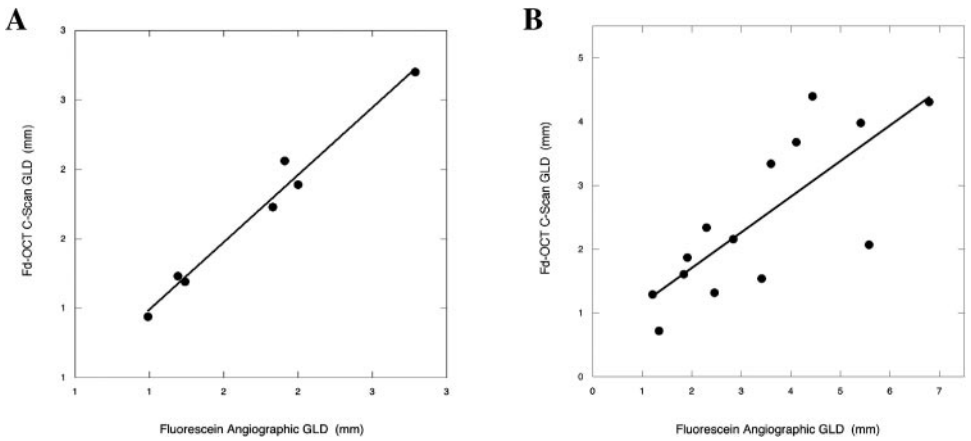

FIGURE 3. Linear regression analysis comparing the size of CNVM associated with eAMD as determined by high-resolution Fd-OCT when compared with FA. (**A**) Analysis of eyes with classic CNVM shows a close linear correlation between GLD of the CNVM obtained by Fd-OCT and that obtained by FA ($r = 0.99$, $F_{1,5} = 214.10$, $P < 0.0001$, $n = 7$). (**B**) Analysis of eyes with nonclassic CNVM showing a less strong but significant correlation between GLD of the CNVM by Fd-OCT with GLD by FA ($r = 0.78$, $F_{1,12} = 18.44$, $P < 0.001$, $n = 14$). The FA GLD was measured, and the Fd-OCT GLD was determined by examining serial reconstructed C-scan images.

Fd-OCT images of the CNVM also allowed us to visualize associated retinal morphologic changes such as CME, SRF, and PED, which may not be well appreciated with FA. Although we hypothesized that occult lesions may be more likely to have an associated PED due to the sub-RPE location of the CNVM and that classic lesions may be more likely to have subretinal fluid due to the subretinal location of the lesion, statistical analysis did not reveal an association. Nonetheless, PED was noted on Fd-OCT in 9 (82%) of 11 eyes with occult CNVM and in none of the eyes with classic CNVM. CME and SRF were frequent findings associated with either growth pattern and most likely result from increased levels of vascular endothelial growth factor (VEGF) associated with both classic and occult CNVMs, which permeates the RPE and affects all the retinal layers.[34,35] The finding was similar to report using Stratus OCT, with which subretinal fluid was noted in all eyes with predominantly classic CNVM and in most eyes with occult CNVM; PED was noted in all eyes with occult CNVM.[16]

There are several limitations to our study that are worth noting. First, although 21 eyes were imaged in total, the number of eyes in each category was small due to the various manifestations of eAMD. Second, since Fd-OCT is a noninvasive technique, there is no histologic correlate to confirm that the highly reflective lesion visualized with Fd-OCT is CNVM. Nonetheless, the highly reflective subretinal and/or sub-RPE lesion seen on Fd-OCT in this and prior studies co-localized to the CNVM seen on FA.[17,28,34,36] Other structural changes associated with CNVM such as subretinal hemorrhage or exudate may appear as highly reflective on Fd-OCT. To minimize this confusion, we limited this study to eyes without concurrent macular hemorrhage. Finally, the classification of the growth pattern of the CNVM on Fd-OCT relies on correctly identifying the RPE layer in the serial B-scans. Making this delineation may be challenging in eyes where there is significant atrophy or disruption of the RPE. Thus, in one eye, the CNVM growth pattern on Fd-OCT was indeterminant.

Despite these limitations, the results of this study demonstrate the potential usefulness of Fd-OCT in visualizing CNVM and studying the growth pattern and associated morphologic changes in eyes with eAMD. With today's trend toward pharmacologic therapy for exudative CNVM, accurate angiographic classification of CNVM is not essential in determining treatment. However, response to pharmacologic therapy is not uniform among patients, and results of previous studies suggest that classic and occult CNVMs may have different prognoses and natural courses.[34,35,37,38] Since angiographic classification of CNVM is not always predictive of the growth pattern of CNVM, further Fd-OCT studies may help determine whether there is a correlation between the growth pattern and morphologic changes associated with CNVM and response to pharmacologic therapy. Unfortunately, this question could not be addressed in our present study, since most of the subjects were imaged before anti-VEGF therapy became the standard of care. Now that Fd-OCT is commercially available, the potential usefulness of Fd-OCT in diagnosing and managing patients with eAMD can be further explored in clinical practice and clinical trials.

References

1. Friedman DS, O'Colmain BJ, Munoz B, et al. for the Eye Diseases Prevalence Research Group. Prevalence of age-related macular degeneration in the United States. *Arch Ophthalmol.* 2004;122:564–572.
2. Green WR, McDonnell PJ, Yeo JH. Pathologic features of senile macular degeneration. *Ophthalmology.* 1985;92:615–627.
3. Green WR. Clinicopathologic studies of treated choroidal neovascular membranes: a review and report of two cases. *Retina.* 1991;11:328–356.
4. Green WR, Enger C. Age-related macular degeneration histopathologic studies. *Ophthalmology.* 1993;100:1519–1535.
5. Grossniklaus HE, Hutchinson AK, Capone A Jr, et al. Clinicopathologic features of surgically-excised choroidal neovascular membranes. *Ophthalmology* 1994;101:1099–1111.
6. Grossniklaus HE, Martinez JA, Brown VB, et al. Immuno-histochemical and histochemical properties of surgically-excised subretinal neovascular membranes in age-related macular degeneration. *Am J Ophthalmol.* 1992;154:464–472.
7. Grossniklaus HE, Green WR, for the Submacular Surgery Trials Research Group. Histopathologic and ultrastructural findings of surgically-excised choroidal neovascularization. *Arch Ophthalmol* 1998;116:745–749.
8. Gass JD. Biomicroscopic and histopathologic considerations regarding the feasibility of surgical excision of subfoveal neovascular membranes. *Am J Ophthalmol.* 1994;118:285–298.
9. Grossniklaus HE, Gass JD. Clinicopathologic correlations of surgically excised type 1 and type 2 submacular choroidal neovascular membranes. *Am J Ophthalmol.* 1998;126:59–69.
10. Bressler SB, Silva JC, Bressler NM, et al. Clinicopathologic correlation of occult choroidal neovascularization in age-related macular degeneration. *Arch Ophthalmol.* 1992;110:827–832.
11. Grossniklaus HE, Wilson DJ, Bressler SB, et al. Clinicopathologic studies of eyes that were obtained postmortem from four patients who were enrolled in the submacular surgery trials: SST Report No. 16. *Am J Ophthalmol.* 2006;141:93–104.
12. Lafaut BA, Bartz-Schmidt KU, Vanden Broecke C, et al. Clinicopathological correlation in exudative age related macular degeneration: histological differentiation between classic and occult choroidal neovascularization. *Br J Ophthalmol.* 2000;84:239–243.
13. Hermans P, Lommatzsch A, Bomfeld N, Pauleikhoff D. Angiographic-histological correlation of late exudative age-related mac-

ular degeneration (in German). *Ophthalmologe.* 2003;100:378–383.

14. Submacular Surgery Trials Research Group. Comparison of 2D reconstructions of surgically excised subfoveal choroidal neovascularization with fluorescein angiographic features: SST report No. 15. *Ophthalmology* 2006;113:279e1–e5.
15. Hughes EH, Khan J, Patel N, et al. In vivo demonstration of the anatomic differences between classic and occult choroidal neovascularization using optical coherence tomography. *Am J Ophthalmol.* 2005;139:344–346.
16. Liakopoulos S, Ongchin S, Bansal A, et al. Quantitative optical coherence tomography findings in various subtypes of neovascular age-related macular degeneration. *Invest Ophthalmol Vis Sci.* 2008;49:5048–5054.
17. Alam S, Zawadzki RJ, Choi S, et al. Clinical application of rapid serial Fourier-domain optical coherence tomography for macular imaging. *Ophthalmology.* 2006;113:1425–1431.
18. Zawadzki RJ, Bower BA, Zhao M, et al. Exposure time dependence of image quality in high-speed retinal in vivo Fourier-domain OCT. In: Manns F, Soederber PG, Ho A, et al., eds. *Ophthalmic Technologies XV*. Bellingham, WA: SPIE, 2005;5688.
19. Menke MN, Dabov S, Sturm V. Features of age-related macular degeneration assessed with three-dimensional Fourier-domain optical coherence tomography. *Br J Ophthalmol.* 2008;92:1492–1497.
20. Landa G, Amde W, Doshi V, et al. Comparative study of intravitreal bevacizumab (Avastin) versus ranibizumab (Lucentis) in the treatment of neovascular age-related macular degeneration. *Ophthalmologica.* 2009;223:370–375.
21. Sayanagi K, Sharma S, Yamamoto T, Kaiser PK. Comparison of spectral-domain versus time-domain optical coherence tomography in management of age-related macular degeneration with ranibizumab. *Ophthalmology.* 2009;116:947–955.
22. Chen Y, Vuong LN, Liu J, et al. Three-dimensional ultrahigh resolution optical coherence tomography imaging of age-related macular degeneration. *Opt Express.* 2009;17:4046–4060.
23. Sayanagi K, Sharma S, Kaiser PK. Photoreceptor status after anti-vascular endothelial growth factor therapy in exudative age-related macular degeneration. *Br J Ophthalmol.* 2009;93:622–626.
24. Witkin AJ, Vuong LN, Srinivasan VJ, et al. High-speed ultrahigh resolution optical coherence tomography before and after ranibizumab for age-related macular degeneration. *Ophthalmology.* 2009;116:956–963.
25. MPS Study Group. Subfoveal neovascular lesions in age-related macular degeneration. Guidelines for evaluation and treatment in the Macular Photocoagulation Study. *Arch Ophthalmol.* 1991;109:1242–1257.
26. Wojkowski M, Leitgeb R, Kowalczyk A, et al. In vivo human retina imaging by Fourier domain optical coherence tomography. *J Biomed Opt.* 2002;7:457–463.
27. Nassif N, Cense B, Park B, et al. In vivo high-resolution video-rate spectral-domain optical coherence tomography of the human retina and optic nerve. *Opt Express.* 2004;12:367–376.
28. Truong SN, Alam S, Zawadzki RJ, et al. High resolution Fourier-domain optical coherence tomography of retinal angiomatous proliferation. *Retina.* 2007;27:915–925.
29. Smith AJ, Telander DG, Zawadzki RJ, et al. High-resolution Fourier-domain optical coherence tomography and microperimetric findings after macula-off retinal detachment repair. *Ophthalmology.* 2008;115:1923–1929.
30. Stopa M, Bower BA, Davies E, Izatt JA, Toth CA. Correlation of pathologic features in spectral domain optical coherence tomography with conventional retinal studies. *Retina.* 2008;28:298–308.
31. Zawinka C, Ergun E, Stur M. Prevalence of patients presenting with neovascular age-related macular degeneration in an urban population. *Retina.* 2005;25:324–331.
32. Olsen T, Feng X, Kasper T, et al. Fluorescein angiographic lesion type frequency in neovascular age-related macular degeneration. *Ophthalmology.* 2004;111:250–255.
33. Margherio RR, Margherio AR, DeSantis ME. Laser treatments with verteporfin therapy and its potential impact on retinal practices. *Retina.* 2000;20:325–330.
34. Rosenfeld PJ, Brown DM, Heier JS, et al. Ranibizumab for neovascular age-related macular degeneration. *N Engl J Med.* 2006;355:1419–1431.
35. Brown DM, Kaiser PK, Michels M, et al. Ranibizumab versus verteporfin for neovascular age-related macular degeneration. *N Engl J Med.* 2006;355:1432–1444.
36. de Bruin DM, Burnes D, Loewenstein J, et al. In-vivo three-dimensional imaging of neovascular age related macular degeneration using optical frequency domain imaging of 1050 nm. *Invest Ophthalmol Vis Sci.* 2008;49(10):4545–4552.
37. Macular Photocoagulation Study Group. Laser photocoagulation of subfoveal neovascular form of age-related macular degeneration: updated findings of two clinical trials. *Arch Ophthalmol* 1993;111:1200–1209.
38. Macular Photocoagulation Study Group. Occult choroidal neovascularization influence on visual outcome in patients with age-related macular degeneration. *Arch Ophthalmol* 1996;114:400–412.